If we divide Eq. (6-9) by $W_j(\nu_j'' - \nu_j')$, we get the general species equation as

$$\nabla \cdot \left[(\rho \mathbf{v}) \frac{Y_j}{W_j(\nu_j'' - \nu_j')} - (\rho \mathscr{D}) \nabla \frac{Y_j}{W_j(\nu_j'' - \nu_j')} \right] = - \frac{\omega_j}{W_j(\nu_j'' - \nu_j')} \equiv -\dot{M} \tag{6-11}$$

Note that in the global reaction, if we let j represent the oxidizer, then

$$\nu_j'' - \nu_j' = -\nu_O' = -\phi_m$$

and if we let j represent fuel, we have

$$\nu_j'' - \nu_j' = -\nu_F' = -1$$

The mass diffusion equation for all the species present in a general system can be put into the same form by setting

$$\alpha_j \equiv \frac{Y_j}{W_j(\nu_j'' - \nu_j')} \tag{6-12}$$

Then Eq. (6-11) reduces to

$$\nabla \cdot \left[(\rho \mathbf{v}) \alpha_j - \rho \mathscr{D} \nabla \alpha_j \right] = -\dot{M} \tag{6-13}$$

Following the Shvab–Zel'dovich formulation given in Section 3.10, we can arrange the energy equation in the following form:

$$\nabla \cdot \left[\rho \mathbf{v} \frac{C_p T}{\Delta H_r W_j(\nu_j'' - \nu_j')} - \frac{\lambda}{C_p} \nabla \frac{C_p T}{\Delta H_r W_j(\nu_j'' - \nu_j')} \right] = \frac{-\omega_j}{W_j(\nu_j'' - \nu_j')} = -\dot{M}$$

Let

$$\alpha_T \equiv \frac{C_p T}{\Delta H_r W_j(\nu_j'' - \nu_j')}$$

then

$$\nabla \cdot \left[(\rho \mathbf{v}) \alpha_T - \rho \mathscr{D} \nabla \alpha_T \right] = -\dot{M} \tag{6-14}$$

Comparing Eq. (6-14) with Eq. (6-13), we notice that both α_j and α_T satisfy the same differential equation.

Equation (6-13) and Eq. (6-14) may both be expressed as

$$L(\alpha) = -\dot{M} \tag{6-15}$$

where the linear operator L is defined by

$$L(\alpha) \equiv \nabla \cdot \left[(\rho \mathbf{v}) \alpha - \rho \mathscr{D} \nabla \alpha \right] \tag{6-16}$$

The inhomogeneous nonlinear rate term may be eliminated from all except one of the relations corresponding to Eq. (6-15). Selecting α_1 to be the dependent variable for the inhomogeneous equation, we have

$$L(\alpha_1) = -\dot{M} \tag{6-17}$$

Other flow variables are then determined by the linear homogeneous equation through the use of coupling functions β:

$$L(\beta) = 0 \tag{6-18}$$

with $\beta = \alpha_T - \alpha_1 \equiv \beta_T$ or $\beta = \alpha_j - \alpha_1 \equiv \beta_j$ $(j \neq 1)$. This procedure is quite important in solving diffusion-flame problems, since in these problems one often finds that by solving the linear equations for relations between flow variables, burning rates may eventually be determined without solving the nonlinear equation. Equation (6-18) is deceptively simple in appearance; it is hard to solve unless additional approximations are made. In general, $\rho \mathbf{v}$ and $\rho \mathscr{D}$ do depend on β_j or β_T; thus the operator L depends implicitly on β, and Eq. (6-18) is actually nonlinear.

1.1 Basic Assumptions and Solution Method

Burke and Schumann assumed that:

1. At port position, the velocities of air and fuel are constant, equal, and uniform across their respective tubes. This is accomplished by varying the radii of the tubes and also the molar fuel ratio which is given by $r_j^2/(r_s^2 - r_j^2)$.
2. The velocity of the fuel and air up the duct in the region of the flame is the same as the velocity at the port (no tube friction loss).
3. $\rho \mathscr{D}$ is constant.
4. Diffusion in the axial direction is negligible in comparison with that in the radial direction:

$$\frac{\partial^2 Y_i}{\partial r^2} \gg \frac{\partial^2 Y_j}{\partial z^2}$$

5. Mixing is caused by diffusion only, and the radial velocity component is equal to zero:

$$v_r = 0$$

6. Reaction takes place at $\phi = 1$ (at the flame surface).

The only differential equation that we need to consider for the mass-fraction distribution is Eq. (6-18):

$$L(\beta) = 0$$

with

$$\beta = \alpha_F - \alpha_O \tag{6-19}$$

$$\alpha_F = \frac{-Y_F}{W_F \nu'_F}, \qquad \alpha_0 = \frac{-Y_O}{W_O \nu'_O} \tag{6-20}$$

In cylindrical coordinates, this differential equation is

$$\left(\frac{v_z}{\mathscr{D}}\right)\frac{\partial \beta}{\partial z} - \frac{1}{r}\frac{\partial}{\partial r}\left(r\frac{\partial \beta}{\partial r}\right) = 0 \tag{6-21}$$

The boundary conditions for Eq. (6-21) are

$$\beta = -\frac{(Y_F)_{z=0}}{W_F \nu'_F} \qquad \text{at} \quad z = 0, \quad 0 \le r \le r_j \tag{6-22}$$

$$\beta = +\frac{(Y_O)_{z=0}}{W_O \nu'_O} \qquad \text{at} \quad z = 0, \quad r_j \le r \le r_s \tag{6-23}$$

and

$$\frac{\partial \beta}{\partial r} = 0 \qquad \text{at } r = 0,\ z > 0, \text{ and at } r = r_s,\ z > 0 \tag{6-24}$$

It is convenient to introduce the dimensionless coordinates

$$\xi \equiv \frac{r}{r_s}$$

$$\eta \equiv \frac{z\mathscr{D}}{v_z r_s^2} \tag{6-25}$$

and to define the reduced parameters

$$C \equiv \frac{r_j}{r_s}$$

$$\nu \equiv \frac{(Y_O)_{z=0} W_F \nu'_F}{(Y_F)_{z=0} W_O \nu'_O} \tag{6-26}$$

and the reduced dependent variable

$$\gamma \equiv \beta \frac{W_F \nu'_F}{(Y_F)_{z=0}} \tag{6-27}$$

In terms of these quantities, Eqs. (6-21) through (6-24) become

$$\frac{\partial \gamma}{\partial \eta} = \frac{1}{\xi}\frac{\partial}{\partial \xi}\left(\xi \frac{\partial \gamma}{\partial \xi}\right), \tag{6-28}$$

$$\gamma = \begin{cases} 1 & \text{at} \quad \eta = 0, \quad 0 \le \xi < C, \\ -\nu & \text{at} \quad \eta = 0, \quad C < \xi < 1, \end{cases} \tag{6-29}$$

$$\frac{\partial \gamma}{\partial \xi} = 0 \qquad \text{at } \xi = 1, \text{ and at } \xi = 0, \quad \eta > 0 \tag{6-30}$$

By the method of separation of variables, it can be shown that a part of the decomposed solution satisfies the Bessel's differential equation of order n:

$$\frac{d^2y}{dx^2} + \frac{1}{x}\frac{dy}{dx} + \left(1 - \frac{n^2}{x^2}\right)y = 0.$$

The functions J_0 and J_1 shown in the accompanying graph are solutions of the above differential equation; they are called the Bessel functions of the first kind (of order 0 and 1 respectively). The mathematical forms of the Bessel functions are

$$J_0(x) = 1 - \frac{x^2}{2^2} + \frac{x^4}{2^4(2!)^2} - \cdots + (-1)^n \frac{x^{2n}}{2^{2n}(n!)^2}$$

$$= \sum_{n=0}^{\infty} (-1)^n \frac{(x/2)^{2n}}{n!n!}$$

and

$$J_m(x) = \sum_{n=0}^{\infty} \frac{(-1)^n x^{m+2n}}{2^{m+2n} n! \Gamma(m+n+1)}, \qquad m > 0$$

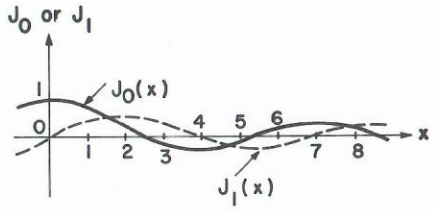

Bessel functions of the first kind of order 0 and 1.

The final solution for γ in power-series form is

$$\gamma = (1+\nu)C^2 - \nu + 2(1+\nu)C\sum_{n=1}^{\infty}\frac{1}{\phi_n}\frac{J_1(C\phi_n)}{[J_0(\phi_n)]^2}J_0(\phi_n\xi)e^{-\phi_n^2\eta} \quad (6\text{-}31)$$

where ϕ_n represent successive roots of the equation $J_1(\phi) = 0$ (with ordering convention $\phi_n > \phi_{n-1}$, $\phi_0 = 0$).

1.2 Flame Shape and Flame Height

If the entire reaction is to occur at a flame surface, then

$$\beta = 0, \quad \text{or} \quad \gamma = 0$$

at the flame surface. Hence, setting $\gamma = 0$ in Eq. (6-31) provides a relation between ξ and η that defines the locus of the flame surface [$\eta = f(\xi)$, or $z = g(r)$]. The shape of the surface obtained in this manner is shown in Fig. 6.1 for two different values of ν.

The flame height is obtained by solving Eq. (6-31) for η after setting $\xi = 0$ for overventilated flames or $\xi = 1$ for underventilated flames (and, of course, $\gamma = 0$ in either case). Since the flame heights are generally large enough to cause the factor $e^{-\phi_n^2\eta}$ to decrease rapidly as n increases at these values of η, it usually suffices to retain only the first few terms of the sum in Eq. (6-31) for this calculation. Neglecting all the terms except $n = 1$, we obtain the rough approximation

$$\eta = \frac{1}{\phi_1^2}\ln\left\{\frac{2(1+\nu)CJ_1(C\phi_1)}{[\nu-(1+\nu)C^2]\phi_1 J_0(\phi_1)}\right\} \quad (6\text{-}32)$$

for the dimensionless flame height of an underventilated flame. The first zero of $J_1(\phi)$ is $\phi_1 = 3.83$. The flame shapes and flame heights obtained from Eq. (6-32) by Burke and Schumann (Fig. 6.3) are in surprisingly good agreement with experiments, considering the drastic nature of some of the assumptions.

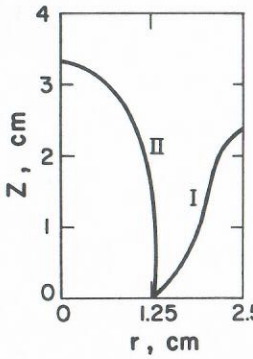

Figure 6.3 Calculated diffusion flame height: curve I, underventilated cylindrical flame; curve II, overventilated cylindrical flame.

In more recent work, Penner and Bahadori[24] and Chung and Law[25] reexamined the Burke-Schumann problem and retained the axial diffusion terms. In Penner and Bahadori's study,[24] they considered diffusion flames with arbitrary transport coefficients and chemical reactions. The closed-form solution obtained is slightly more complex than that of Burke and Schumann.[1] In Chung and Law's work,[25] the solution was obtained by a perturbation method under the assumption that the Lewis number is very close to unity. The zeroth order solution was obtained by separation of variables, and the 1st order problem was solved using Green's functions. Their results showed that the flame is made longer and narrower by including streamwise diffusion transport. They also showed that the Burke-Schumann solution is generally valid for large Padet numbers.

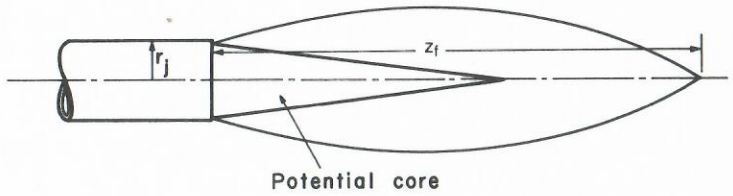

Horizontal laminar fuel jet.

2 PHENOMENOLOGICAL ANALYSIS OF FUEL JETS

In the following, we shall use a simple phenomenological approach to show that for a laminar flame, the flame height is proportional to the volumetric flow rate and inversely proportional to the mass diffusivity:

$$(z_f)_{\text{laminar}} \propto \frac{\text{volumetric flow rate}}{\mathscr{D}} \quad (6\text{-}33)$$

For a turbulent flame

$$(z_f)_{\text{turbulent}} \propto \text{port size} \quad (6\text{-}34)$$

Sometimes very useful information can be obtained from simple phenomenological reasoning. The fundamental assumption which has been made here is that the combustion process does not affect the mixing rate between the fuel jet and the surrounding oxidizer. In essence, as soon as the oxidizer mixes into the fuel, it reacts. We have considered a simple cylindrical problem; thus as soon as the oxidizer has diffused from the jet edge to the center, we have completely burned the fuel—or, in other words, we have the flame height.

Our problem is simply one of the laminar diffusional mixing of a jet—which in itself can be approached phenomenologically. Simple kinetic theory tells us that in molecular diffusion the average displacement of a molecule is given by

$$\frac{1}{2}\frac{d\overline{X}^2}{dt} = \mathscr{D} \quad (6\text{-}35)$$

where $\mathscr{D} = \frac{1}{2}\bar{u}l$ is the molecular diffusion coefficient and $\overline{X}^2$ is the mean square of the displacement of the particle in a specified direction in the time t. To arrive at an estimate of the flame length, it is proposed to use this equation

from kinetic theory in the integrated form

$$\xi^2 = 2\mathscr{D}t \tag{6-36}$$

where ξ^2 denotes the mean squared displacement of a molecule from its initial location due to diffusion during time t. The length of the flame is assumed to correspond to the condition that at the point on the stream axis where combustion is complete, the average depth of penetration of air into fuel must be approximately equal (or proportional, if one likes) to the radius of the burner tube. As an approximation, ξ is identified with the average depth of penetration. The gas velocity $\overline{V}$ (inside the port) is taken as constant, so that the time t required for completion of the diffusion process—which is the time in which a gas element flows from the burner port to the flame tip—is given by

$$t = \frac{z_f}{\overline{V}} \qquad \text{(residence time)} \tag{6-37}$$

The radial diffusion time can be approximated by $\xi^2/2\mathscr{D}$ or $r_j^2/2\mathscr{D}$. Assuming that the residence time is of the same order of the diffusion time, we have

$$z_{f,L} \propto \frac{r_j^2\overline{V}}{2\mathscr{D}} \propto \frac{(\pi r_j^2)\overline{V}}{2\pi\mathscr{D}} \propto \frac{\text{volumetric flow rate}}{\mathscr{D}} \tag{6-38}$$

This result is significant; it clearly indicates that for laminar-diffusion flames the height is proportional to the volumetric flow rate, and inversely proportional to the mass diffusivity. The relationship is also helpful for studying turbulent fuel jets, as explained in the following simple analysis.

First, let us recall that the Schmidt number is defined as $\nu/\mathscr{D}$. For constant Schmidt number, we have $\mathscr{D} \propto \nu$. Hence, Eq. (6-38) can be rewritten as

$$z_{f,L} \propto \frac{r_j^2\overline{V}}{\nu}$$

For the turbulent case, we use the same reasoning to arrive at a relationship similar to the above, except that instead of the molecular viscosity ν, we must use the turbulent eddy viscosity ν_t in the denominator, since $\nu_t \gg \nu$. Thus,

$$z_{f,T} \propto \frac{r_j^2\overline{V}}{\nu_t} \tag{6-39}$$

Note that $\nu_t \propto lu'_{\text{rms}}$, where l is the scale of turbulence and is proportional to the tube diameter (or tube radius) and u'_{rms} is the intensity of turbulence, which is approximately proportional to the mean flow velocity at the axis; thus,

$$\nu_t \propto r_j\overline{V} \tag{6-40}$$

Combining the Eqs. (6-39) and (6-40), we have

$$z_{f,T} \propto \frac{r_j^2\overline{V}}{r_j\overline{V}} \propto r_j \tag{6-41}$$

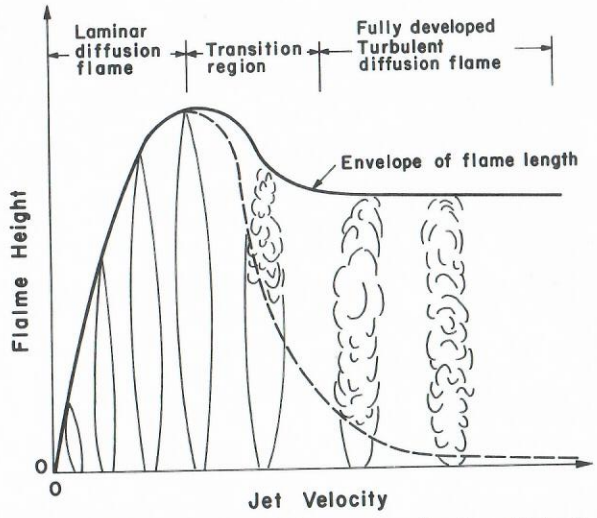

Figure 6.4 The variation of flame height and character as a function of jet velocity (after Hottel and Hawthorne[2]).

This says that the height of a turbulent-diffusion flame is proportional to the port radius only. It is a very important practical conclusion that has been verified in many ways. The variation of diffusion flame height as a function of jet velocity is shown in Fig. 6.4. The laminar-diffusion height follows the functional dependence shown in Eq. (6-38), while the turbulent-diffusion height follows Eq. (6-41). More discussion of turbulent diffusion-flame structure is given in Chapter 7.

3 LAMINAR DIFFUSION FLAME JETS

Injection of fuel jets into a combustor containing oxidizers is a common practice in many combustion systems such as diesel engines, gas-turbine engines, industrial furnaces, and ramjet engines. Under the condition when there is no cross-flow or buoyancy effect and also the fuel jet and the ambient air are parallel, the diffusion flame is essentially the same as the Burke–Schumann laminar-diffusion flame we discussed in Section 2. The only difference is that the effect of the outer tube becomes negligible when the combustor diameter becomes very large in comparison with the fuel-jet diameter. The schematic diagram of a single fuel jet under the above condition is shown in Fig. 6.5*a*. When the buoyancy or cross-flow effect is significant, the flame geometry and the boundary of the hot gases will not be axisymmetric (see Fig. 6.5*b*). Before we study the detailed structure of these diffusion flames, we shall provide some background on laminar jet mixing.

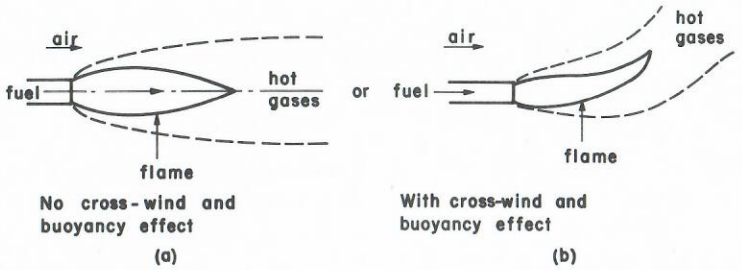

Figure 6.5 Laminar diffusion flame jets (*a*) without and (*b*) with cross-wind and buoyancy effect.

3.1 Laminar Jet Mixing

Consider a gaseous fuel jet with a uniform (top-hat) velocity profile issuing from a circular hole of radius r_0 into quiescent air. Mixing will occur between the gaseous fuel jet and ambient air as shown in Fig. 6.6. At some downstream location, the velocity profile will have a maximum at the centerline and a gradual decay to zero at the boundary of the mixing zone. The air is entrained through the boundary of the mixing zone. For simplicity of analysis, let us make the following assumptions:

1. The surrounding air far from the jet is at rest.
2. Chemical reaction is absent.
3. ρ, μ and other properties of the gases are uniform (uniform property flow).
4. The flow is steady.
5. The effect of buoyancy is absent.
6. The pressure in the fluid is uniform.

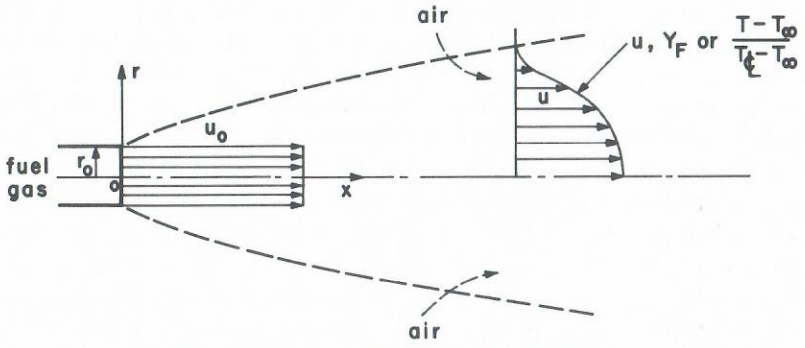

Figure 6.6 Velocity and concentration profile distributions in a laminar jet.

7. Mass diffusion, heat conduction, and viscous action in the axial direction are negligible.
8. Sc = Pr = 1.

The overall mass conservation equation can be written as

$$\frac{\partial}{\partial x}(\rho u r) + \frac{\partial}{\partial r}(\rho v r) = 0 \tag{6-42}$$

The x-momentum equation is

$$\frac{\partial}{\partial x}(\rho u r u) + \frac{\partial}{\partial r}(\rho v r u) = \frac{\partial}{\partial r}\left(\mu r \frac{\partial u}{\partial r}\right) \tag{6-43}$$

The fuel species conservation equation written in terms of mixture fraction, f, is

$$\frac{\partial}{\partial x}(\rho u r f) + \frac{\partial}{\partial r}(\rho v r f) = \frac{\partial}{\partial r}\left(\rho \mathscr{D} r \frac{\partial f}{\partial r}\right) \tag{6-44}$$

where the mixture fraction has been defined in Section 8 of Chapter 1. Taking ρ, μ and $\mathscr{D}$ to be uniform and applying the assumptions that Sc = Pr = Le = 1, the above equations can be reduced to

$$\frac{\partial u}{\partial x} + \frac{\partial v}{\partial r} + \frac{v}{r} = 0 \tag{6-45}$$

$$u\frac{\partial u}{\partial x} + v\frac{\partial u}{\partial r} = \frac{\nu}{r}\frac{\partial}{\partial r}\left(r\frac{\partial u}{\partial r}\right) \tag{6-46}$$

$$u\frac{\partial f}{\partial x} + v\frac{\partial f}{\partial r} = \frac{\nu}{r}\frac{\partial}{\partial r}\left(r\frac{\partial f}{\partial r}\right) \tag{6-47}$$

The boundary conditions at the entrance station are

$$x=0, \quad r \le r_0: \qquad u = u_0 \tag{6-48}$$

$$f = 1 \tag{6-49}$$

$$x=0, \quad r > r_0: \qquad u = 0 \tag{6-50}$$

$$f = 0 \tag{6-51}$$

At large radius, one has

$$r \to \infty: \qquad u = 0 \tag{6-52}$$

$$f = 0 \tag{6-53}$$

There are two jet invariants based upon the conservation of momentum and species. These jet invariants are defined as follows:

$$I_u \equiv \frac{1}{\nu}\int_0^\infty u^2 r\,dr = \frac{1}{\nu}\left(\tfrac{1}{2}u_0^2 r_0^2\right) \tag{6-54}$$

$$I_f = \frac{1}{\nu}\int_0^\infty ufr\,dr = \frac{1}{\nu}\left(\tfrac{1}{2}u_0 r_0^2\right) \tag{6-55}$$

According to Spalding[3] and Schlichting,[4] the following equations satisfy the governing partial differential equations and boundary conditions at the far field:

$$u = \frac{3}{4}\frac{I_u}{x}\left(1 + \frac{\xi^2}{4}\right)^{-2} \tag{6-56}$$

or

$$\frac{u}{u_0} = \frac{3}{32}\left[\frac{\mathrm{Re}_{d_0} d_0}{x}\right]\left(1 + \tfrac{1}{4}\xi^2\right)^{-2} \tag{6-56a}$$

$$v = \left(\tfrac{3}{8}I_u\nu\right)^{1/2}\frac{\xi}{x}\left(1 - \frac{\xi^2}{4}\right)\left(1 + \frac{\xi^2}{4}\right)^{-2} \tag{6-57}$$

or

$$\frac{v}{u_0} = \frac{\sqrt{3}}{8}\frac{d_0}{x}\left(\xi - \tfrac{1}{4}\xi^3\right)\left(1 + \tfrac{1}{4}\xi^2\right)^{-2} \tag{6-57a}$$

and

$$f = \frac{3}{4}\frac{I_f}{x}\left(1 + \frac{\xi^2}{4}\right)^{-2} \tag{6-58}$$

where the dimensionless variable ξ is defined as

$$\xi \equiv \left(\frac{3}{8}\frac{I_u}{\nu}\right)^{1/2}\frac{r}{x} = \frac{\sqrt{3}}{8}\left(\frac{r}{d_0}\right)\left[\frac{\mathrm{Re}_{d_0} d_0}{x}\right] \tag{6-59}$$

It is quite evident from the above solution that the velocity and concentration profiles are self-similar; that is, they depend upon r/x alone. Based upon Eqs. (6-56) and (6-58), the centerline values of u and f are

$$u_{\text{℄}}\,x = \tfrac{3}{4}I_u$$

$$f_{\text{℄}}\,x = \tfrac{3}{4}I_f \tag{6-60}$$

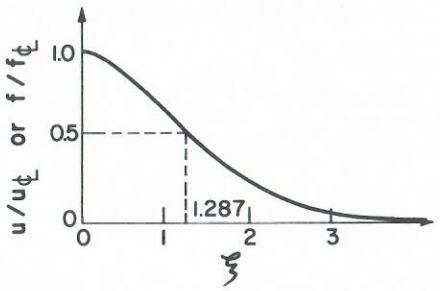

Figure 6.7 Similarity profile of velocity or concentration as a function of dimensionless variable.

Since the centerline velocity is less than the jet exit velocity ($u < u_0$) and also the mixture fraction at the centerline in the downstream location is less than one, we can conclude from Eq. (6-60) that the x-value satisfying the above far-field solution must obey the following inequality:

$$x > \frac{3}{4}\frac{I_u}{u_0}, \quad \text{or} \quad \frac{x}{r_0} > \frac{3}{8}\frac{u_0 r_0}{\nu} \tag{6-61}$$

The radial profiles of u and f, when normalized by their respective centerline values, are

$$\frac{u}{u_{\text{℄}}} = \frac{f}{f_{\text{℄}}} = \frac{1}{\left(1 + \tfrac{1}{4}\xi^2\right)^2} \tag{6-62}$$

The sketch shown in Fig. 6.7 represents the velocity or concentration profiles qualitatively. It should be noted that

$$\frac{u}{u_{\text{℄}}} = 0.5 \qquad \text{for} \quad \xi = 1.287.$$

The radius at which the velocity has one-half of its centerline velocity is denoted $r_{1/2}$. From Eq. (6-59), we have

$$\frac{r_{1/2}}{x} = 1.287\left(\frac{8\nu}{3I_u}\right)^{1/2} = 2.97\frac{\nu}{u_0 r_0} \tag{6-63}$$

This equation implies that the angle of the spreading of the jet is inversely proportional to the Reynolds number.

The total mass flow rate in the jet, $\dot{m}$, can be obtained from the following integration:

$$\dot{m} \equiv \int_0^\infty 2\pi r\rho u\,dr \tag{6-64}$$

Substituting Eq. (6-56) into Eq. (6-64) and carrying out the integration, we have

$$\dot{m} = 2\pi\rho x^2\left(\frac{8}{3}\frac{\nu}{I_u}\right)\left(\frac{3}{4}\frac{I_u}{x}\right)\int_0^\infty \frac{\xi\, d\xi}{\left(1+\frac{1}{4}\xi^2\right)^2} = 8\pi\mu x \tag{6-65}$$

The entrainment rate can be obtained by differentiating Eq. (6-65), i.e.,

$$\frac{d\dot{m}}{dx} = 8\pi\mu \tag{6-66}$$

Associated with the entrainment process, an entrainment velocity can be defined by

$$v_{\text{ent}} \equiv -\frac{1}{2\pi r_{jb}\rho}\frac{d\dot{m}}{dx} = \frac{-4\mu}{r_{jb}\rho} = -4\frac{\nu}{r_{jb}} \tag{6-67}$$

where r_{jb} represents the radius at the jet boundary. In dimensionless form, Eq. (6-57) can be written as

$$\frac{v}{v_{\text{ent}}} = -\frac{\sqrt{3}}{16}\frac{u_0 r_0}{\nu}\frac{\xi}{x}\left(1-\frac{\xi^2}{4}\right)\left(1+\frac{\xi^2}{4}\right)^{-2} r_{jb} \tag{6-68}$$

According to Schlichting,[4]

$$r_{jb} \approx \frac{16}{\sqrt{3}}\left(\frac{x}{\text{Re}_{d_0} d_0}\right) d_0 \tag{6-69}$$

Using the above expression, the radial velocity can be expressed as

$$\frac{v}{v_{\text{ent}}} = -\tfrac{1}{4}\xi^2\left(1-\frac{\xi^2}{4}\right)\left(1+\frac{\xi^2}{4}\right)^{-2} \tag{6-70}$$

It is interesting to note that at large ξ, $v/v_{\text{ent}} \to 1$ and at small ξ, $v/v_{\text{ent}} \sim -\xi^2/4$.

The equations describing lines of constant u and f can be found by rearranging Eq. (6-56) or (6-58).

$$r = \frac{16}{\sqrt{3}}\frac{x}{\text{Re}_{d_0}}\sqrt{\sqrt{\frac{3}{32}\left(\frac{\text{Re}_{d_0} d_0}{x}\right)\frac{u_0}{u}} - 1} \tag{6-71}$$

where

$$\text{Re}_{d_0} \equiv \frac{u_0 d_0}{\nu}$$

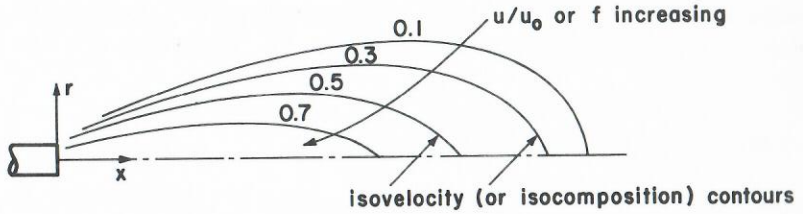

Figure 6.8 Isovelocity or isocomposition contours of a laminar jet.

Curves obeying Eq. (6-71), for fixed values of u/u_0 (or f), have the form shown in Fig. 6.8.

Since there is exact similarity between the processes of mass transfer and momentum transfer, we can write

$$f = \frac{u}{u_0} \tag{6-72}$$

If we further assume that Le = 1 and consider the energy equation, we find that the temperature field is related to the concentration field by

$$\frac{T - T_\infty}{T_0 - T_\infty} = f \tag{6-73}$$

Thus, the curves in Fig. 6.8 can also be interpreted as isotherms.

If the Schmidt number is not equal to unity but equal to some constant, then one can show that

$$\frac{f}{f_{\text{℄}}} = \left(\frac{u}{u_{\text{℄}}}\right)^{\text{Sc}} \tag{6-74}$$

This equation implies that for Sc < 1, the concentration profile is broader than the velocity profile. It should also be noted that, under this condition, the centerline mixture fraction $f_{\text{℄}}$ is smaller than that with Sc = 1. Furthermore, the $f_{\text{℄}}$ for Sc ≠ 1 no longer obeys Eq. (6-60).

It is worthwhile to point out that when μ, ρ, and $\mathscr{D}$ vary with f and T, the analytical solution of the governing equations ceases to be possible, and we must adopt numerical methods. Under these circumstances, the quantitative values will be different from those with constant transport properties; however, no qualitative change in the behavior of the jet is anticipated.

The buoyancy effect may be important in some cases. For upward vertical jets with the density of the injected fluid lower than that of the surroundings, buoyancy effects can cause the momentum flux in the jet to increase with vertical distance. Also, when buoyancy forces have components at right angles

to the jet axis, the flow will no longer be axisymmetric. The solutions of these problems are more complex and one usually has to rely upon numerical methods.

3.2 Laminar Jet with Chemical Reactions

In many industrial furnaces, flares, and combustors of propulsive devices, one needs to predict the shape and structure of the diffusion flame resulting from the injection of fuel gases into an oxidizing atmosphere. In order to achieve good predictive ability, the laminar diffusion flame jets must be modeled. Let us consider a steady, axisymmetric, vertical laminar jet with low Mach number but fast chemical reaction rates. We further assume that the pressure is uniform and the buoyancy effect is negligible. Under these specified conditions, the governing differential equations are given as follows:

Continuity (overall) equation:

$$\frac{\partial}{\partial x}(\rho u r) + \frac{\partial}{\partial r}(\rho v r) = 0 \tag{6-75}$$

Axial-momentum conservation equation:

$$\frac{\partial}{\partial x}(\rho u r u) + \frac{\partial}{\partial r}(\rho v r u) = \frac{\partial}{\partial r}\left(\mu r \frac{\partial u}{\partial r}\right) \tag{6-76}$$

Fuel species continuity equation:

$$\frac{\partial}{\partial x}(\rho u r Y_F) + \frac{\partial}{\partial r}(\rho v r Y_F) = \frac{\partial}{\partial r}\left(\rho \mathscr{D}_F r \frac{\partial Y_F}{\partial r}\right) + r\omega_F \tag{6-77}$$

Oxidant species continuity equation:

$$\frac{\partial}{\partial x}(\rho u r Y_O) + \frac{\partial}{\partial r}(\rho v r Y_O) = \frac{\partial}{\partial r}\left(\rho \mathscr{D}_O r \frac{\partial Y_O}{\partial r}\right) + r\omega_O \tag{6-78}$$

Energy-conservation equation:

$$\frac{\partial}{\partial x}(\rho u r h) + \frac{\partial}{\partial r}(\rho v r h) = \frac{\partial}{\partial r}\left(\lambda r \frac{\partial T}{\partial r}\right) + (\Delta H_r)\frac{\partial}{\partial r}\left(\rho \mathscr{D}_F r \frac{\partial Y_F}{\partial r}\right) \tag{6-79}$$

where

$$h \equiv C_p T + Y_F \Delta H_r \tag{6-80}$$

and ΔH_r is the heat of reaction per mass of fuel.

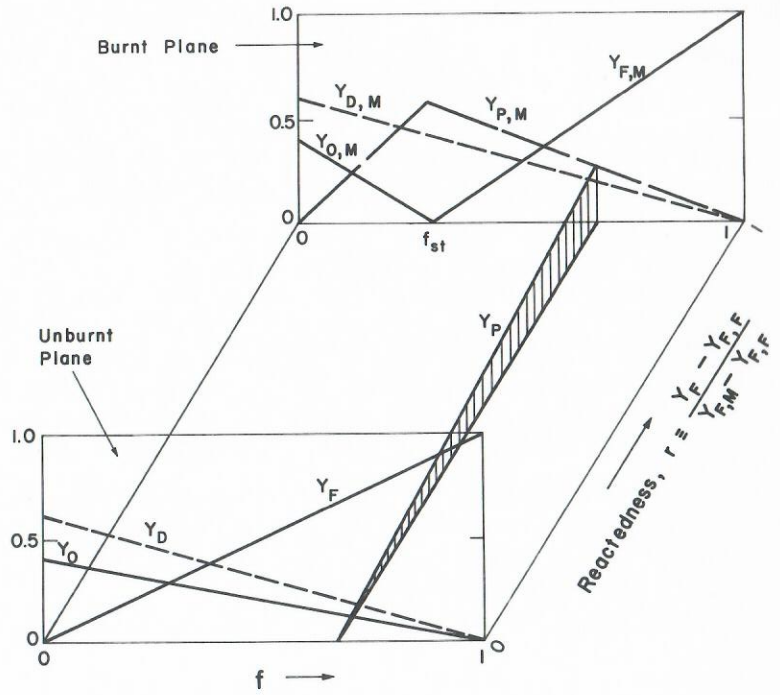

Figure 6.9 Sketch of the mixture state as a function of mixture fraction and reactedness.

To facilitate our discussion and theoretical solution, let us define a term introduced initially by Spalding[3] for many combustion problems: in a *simple chemically reacting system* (SCRS), the pure fuel and pure oxidant are imagined to always unite in fixed proportions, the specific heats of all components are equal, and the transport properties are equal at any point in the mixture but need not be uniform. For such systems, a sketch of mixture state as a function of mixture fraction and reactedness is shown in Fig. 6.9. The symbols $Y_{F,F}$ and $Y_{F,M}$ in Fig. 6.9 represent the mass fractions of fuel in the fuel stream and in the burned mixture stream respectively.

If the fuel and the oxidizer are presumed to form a SCRS, one can relate the rate of production of fuel to that of oxidizer by

$$\omega_F = \left(\frac{F}{O}\right)_{st} \omega_O \tag{6-81}$$

Since $\nu = \mathscr{D} = \alpha$ for a SCRS, so that Sc = Pr = Le = 1, then Eqs. (6-77) and (6-78) can be combined to form

$$\frac{\partial}{\partial x}(\rho u r \zeta) + \frac{\partial}{\partial r}(\rho v r \zeta) = \frac{\partial}{\partial r}\left(\mu r \frac{\partial \zeta}{\partial r}\right) \tag{6-82}$$